Volume 7 No. 6, Dec 2019

Transactions on Networks and Communications

ISSN: 2054-7420

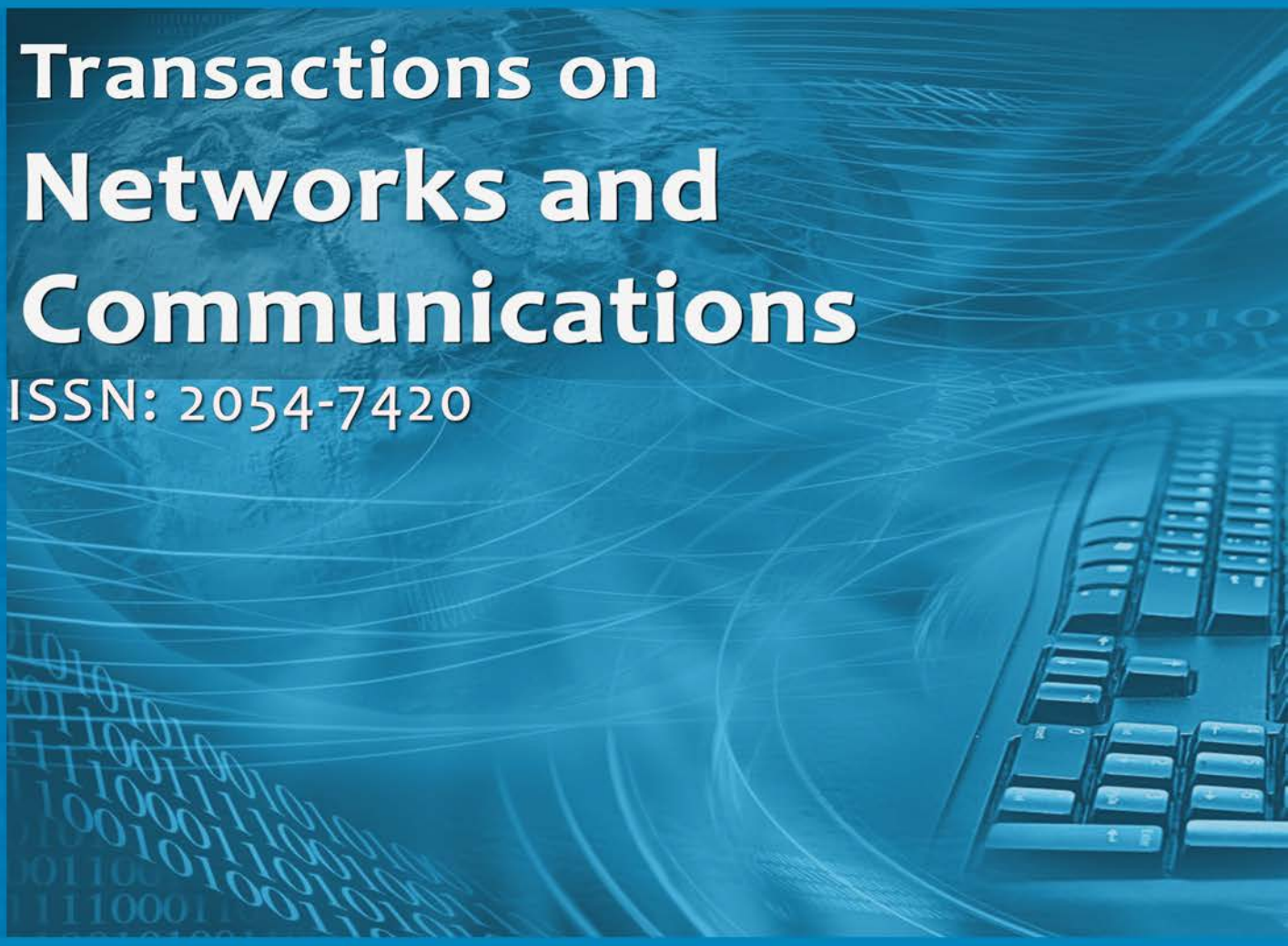

Society for Sciences and Education - United Kingdom

TABLE OF CONTENTS

DISCLAIMER

All the contributions are published in good faith and intentions to promote and encourage research activities around the globe. The contributions are property of their respective authors/owners and the journal is not responsible for any content that hurts someone's views or feelings etc.

SOCIETY FOR SCIENCE AND EDUCATION
UNITED KINGDOM

TNC TRANSACTIONS ON NETWORKS AND COMMUNICATIONS

VOLUME 7, NO. 6
ISSN: 2054 -7420

Study of Miniaturizaption of a Silicon Vapor Chamber for Compact 3D Microelectronics, via a Hybrid Analytical and Finite Element Method

[1] Ma Yue, [2]Shirazy Mahmoud, [1,2,3,4] Struss Quentin, [3] Coudrain Perceval. [4]Colonna Jean-Phulippe, [1] Souifi Abdelkader, [2]Fréchette Luc and [1,5] Gontrand Christian

[1] INL/INSA Lyon, Université de Lyon, 7 avenue Jean Capelle 69621 Villeurbanne, France
[2]UMI-LN2, Université de Sherbrooke, 2500, boul. de l'Université, Sherbrooke (Québec), Canada, J1K 2R1
[3]STMicroelectronics, 850 rue Jean Monnet 38926 Crolles, France
[4] CEA-LETI, MINATEC Campus F-38054 Grenoble, France
[5] IEP2/INSA Fès, Euro-Mediterraneean University of Fès, Marocco
yue.ma@insa-lyon.fr; christian.gontrand@insa-lyon.fr

ABSTRACT

The interest in silicon vapor chambers (SVCs) has increased in the recent years as they have been identified as efficient cooling systems for microelectronics. They present the advantage of higher thermal conductivity and smaller form factor compared to conventional heat spreaders. This work aims to investigate the potential miniaturization of these devices, preliminary to integration on the backside of mobile device chips, located as close as possible to hotspots. While detailed numerical models of vapor chamber operation are developed, an easy modeling with low computational cost is needed for an effective parametric study. Based on the study of the operating limits, this paper shows the thinning potential of a water filled micropillar for a device operating below 10 W and identify the corresponding vapour core height, and wick thickness.

Keywords: Heat Pipe; Hot spots, Finite Element Method; MNR;Imager.

1 Introduction

The generation of heat in the circuits became, in a few decades, the factor more limiting in the continuation of the improvement of the performances of the integrated devices for mobile telephony and the wandering applications. The heat, generated in the active zones of the chips, on the transistor level, is all the more concentrated that the latter are miniaturized. The heat flows generated in the last generations of silicon processors reach orders of magnitude comparable with those of the existing energy systems. The question of thermal dissipation for the electronic systems arises since their emergence. It drained an important research task through five essential technological eras:

HVAC era (1945-1975) (extraction of the hot air Rack Cooling era (1975-1985) (forced convection Liquid/Refrigerant Cooling era (1980-1990), Enhanced Air Cooling era (1985-2000) Nanoelectronics era (2000-currenthly): logic sub-100nm CMOS

DOI: 10.14738/tnc.76.7569
Publication Date: 28th Dec 2019
URL: http://dx.doi.org/10.14738/tnc.76.7569

This last era, known as of nano-electronics, is associated to the presence of localized hot points, in particular at the places of strong densities of calculation in the logical cores, and the emergence of stackings of homogeneous and heterogeneous chips. These tendencies are reinforced in the cases of carry forward per flip-chip, and a fortiori in the schemes of three-dimensional integration (3D-IC). In this last case, indeed, the silicon layers are not only finer but are also insulated between them and are isolated from substrate (BGA or PCB).

The dissipation of generated heat becomes a need which takes multiple scales. Better a conduction is required via optimized materials of interface (Thermal Materials - TIM Interfaces). The use of wasteful passive layers (heat-spreaders) is common [1-2]: their role is to set out again the heat generated by a hot point on greatest possible surface in order to minimize the impact of it. Finally, the natural and forced improvement of the convections is obtained thanks to active systems like heat sinks or ventilators (Figure 1)[3].

The whole of these technological solutions aims at extracting the heat generated in the chips. A second axis of very important work, these last years, consists in designing the chips in a more effective way compared to thermal dimension. Thermal models can thus be integrated into DK-like with the tools of floorplaning for an either electronic or thermoelectric design[4-10]:.

2 Thermal management in the systems strongly integrated/wandering

2.1 Thermal resistance Model

Because of high compactness of the wandering systems such as the tactile telephones or tablets, the capacity to dissipate heat is limited to a few Watts only; the integration of heat-sinks or ventilators being incompatible with the requirement of the thickness reduction. So, this limitation results concretely in two problems of a thermal nature: the high average temperature of the system, and the presence of hot points associated to a dense logical building blocks

The variations in temperature related to the hot points induce important variations in the performances of the devices between two zones of the same chip [11-19]. If it is about a sensor of images CMOS for example, the non-uniformity of temperature within the matrix of pixels can have important consequences on the final quality of the image. As example, the dark current of the pixels doubles for a rise in 6 to 8 degrees. In addition, the engineers must from now on circumvent the risks induced by these hot points by limiting the intense working lives of calculation. In the case of processors multi-hearts, for example, the activity of calculation is sometimes limited to a few tens of millisecond, time to the end of which the acceptable maximum temperature is reached. It is then necessary to stop the activity of the heart so that the system finds an acceptable temperature. The heat generated by a chip can also impact the performances of the surrounding chips in the system . Finally, the lifespan of the chips decreases because of exacerbation of the thermically activated modes of failure.

Before detailing the analytical-numerical structure of our model, we first study the relationship between thermal resistances, both for understanding the model itself and for interpreting the results. As shown in Fig. 1, heat passes through various thermal resistances when it flows from the heat source to the cooling fluid and essentially corresponds to Garimella *et al.* model [20- 22]

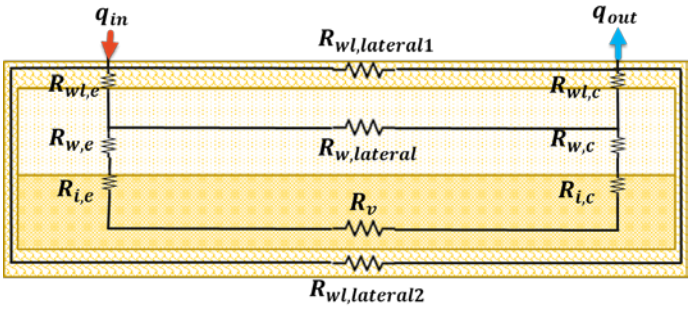

Figure 1 Schematic of approximate network of thermal resistance of FHP

Due to the primary heat transfer processes in each part of the heat pipe, the temperature drop can be represented using the simple effective heat resistance network as shown in Figure 1. Thermal conduction through the wall , inducing thermal resistances, in the evaporator ($R_{wl,e}$) and condenser ($R_{wl,c}$); implies that sections are negligible (cf. the thin thickness of wall), which is targeted at ultrathin heat pipes constructed from high-conductivity materials. Lateral conduction along the heat pipes wall is shown as $R_{wl,lateral1}$ and $R_{wl,lateral2}$; These resistances can be calculated using an effective device length, which reflects the varying heat load throughout the vaporizer and capacitor section and gives::

$$L_{eff} = L_a + \frac{L_e + L_c}{2} \tag{1}$$

The resistances through the wick in the evaporator ($R_{w,e}$) and condenser ($R_{w,c}$) and laterally through the wick ($R_{W,\ lateral}$), are considered as convective only. Convective heat treatment in the porous medium is negligible because of the wall in the 1-D; an efficient saturated wick thermal conductivity is used. The low-temperature, high-conductivity wick's geometry, has resulted in a high strength lateral heat flow. The interfacial phase-change thermal resistances at the wick–vapor interface in the evaporator and condenser sections, indicated by $R_{i\ e}$ and $R_{i,\ c}$, is generally small, then neglected.

The effective thermal resistance of the R_v steam core, calculated by representing the vapor flow field as non-compressible, laminar, full flow between parallel plates, and controlled by continuum physics, to estimate the pressure fall on the core steam over effective length. This decrease is associated with a decrease in saturation temperature by applying the Clapeyron equation and the ideal gas law. According to this approach, effective thermal conductivity is defined for a 1-D lateral resistance along the effective length of vapor:

$$k_{eff,v} = \frac{h_{fg}^2 P_v \rho_v t_v^2}{12 R \mu_v T_v^2} \tag{2}$$

where the thermo -physical properties are evaluated for saturated vapor at the local steam temperature, which changes along the device. To achieve heat loss steam properties, the 1-D steam thermal resistance is discretized and each resistor element is calculated from condenser-side temperature and is repeated in the heat flowing through the steam core. This approach does not take into account convection in the vapor core.

We then obtain an effective heat pipe resistance.

$$R_{HP} = \frac{1}{\frac{1}{R_{wl,lateral1}} + \frac{1}{R_{wl,lateral2}} + \frac{1}{(R_v + R_{w,e} + R_{w,c})}} \tag{3}$$

2.1.1 Performance-limiting Conditions

Comparing the performance between the different input heat streams and different geometries, it is possible to identify the restrictive conditions for weak thickness and low input power. Figure 2 shows the contour map of the ratio between the heat pipe and copper heat spreader thermal resistances with the adiabatic length of heat dissipation and the total thickness. The colored area shows the beneficial heat pipe performance and is whitened as the ratio transitions in favor of copper heat spreader. Performance thresholds and capillary limits are also defined. The pressure of 2250 Pa is then considered the maximum pressure, for capillarity.

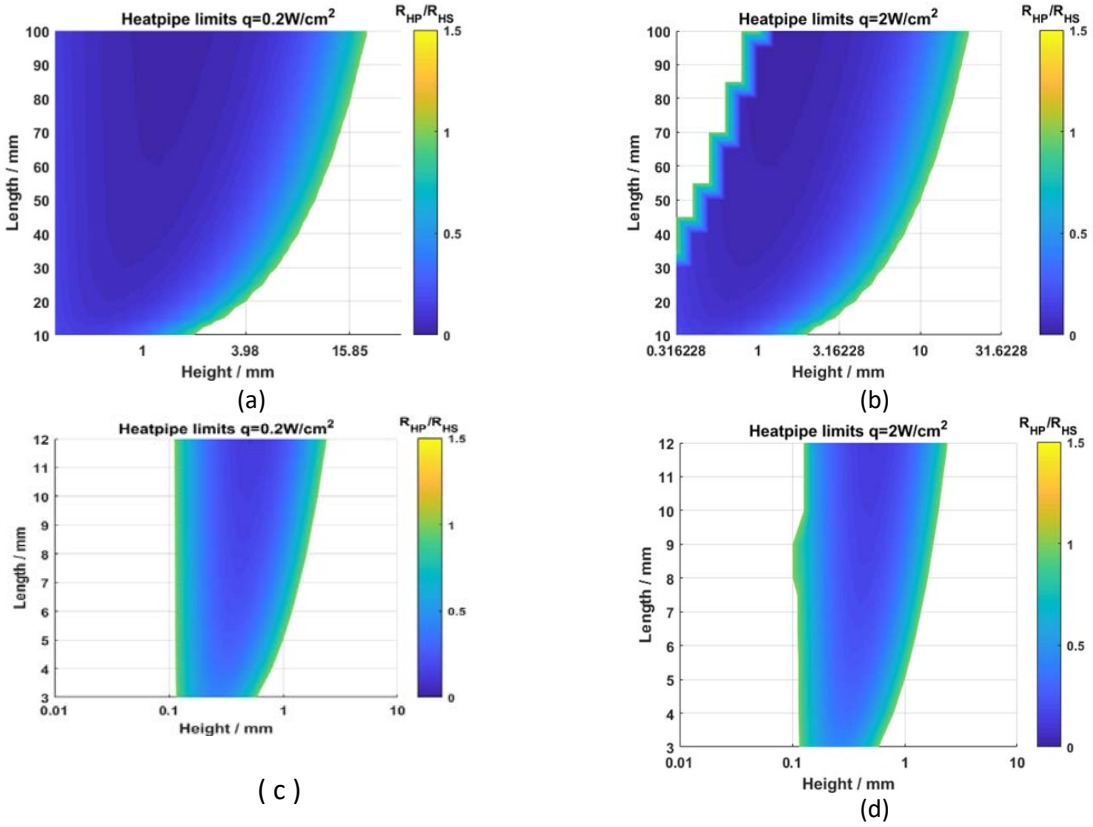

Figure 2 Contour map of the resistance ratio R_{HP}/R_{HS} plotted as a function of adiabatic length and thickness for an input heat flux of (a) 0.2 and (b) 2 W/cm2 for length from 10mm to 100mm, of (c) 0.2 and (d) 2 W/cm² for length from 3mm to 12mm

In Figure 2 (a) (c), show the limiting conditions for the case of a much lower input heat flux of 0,2 W / cm². At low input heat fluxes, there is sufficient capillary pressure due to the reduced fluid velocities, and the capillary limit dramatically shifts to lower thicknesses and higher working lengths.

Figure 2 (b) (d)) illustrate the resistance ratio contour plot for a high input heat flux of 2 W/cm² to show the limits reached when designing very thin heat pipes for weak power dissipation.

For weak thicknesses and with a relatively high temperature flux, the minimum thickness for which RHP/RHS is greater than unity, is governed by the limit of capillary; The advantage of heat pipe performance lies in the small resistances caused by the phase change. This benefit is lost for short, thick

heatpipes that reduce effective length and solid heat pipe spreaders provide with a more direct thermal conductivity path than the heat pipe wick.

Except for the thickness-to-length ratio and the capillary limit, there is another limit, which is called a steam-resistance threshold. This threshold is due to the increasing pressure loss (and corresponding drop in saturation temperature) along the steam core. By replacing the different heat resistance components and representing the thicknesses of the cores, wick vapor and walls as the whole thickness fraction, ie $t_v = r_v t$, $t_w = r_w t$ and $t_{wl} = r_{wl} t$, the threshold conditions can be written as[21]:

$$\frac{r_w}{k_w}\left(\frac{1}{L_e}+\frac{1}{L_c}\right)t^4 - \frac{L_{eff}}{k_s}\frac{1}{1-r_w}t^2 + \frac{L_{eff}}{M_v r_v^3} = 0 \tag{4}$$

The solution of the equation translates into two positive roots that represent the thickness in both threshold states (vapor resistance and high ratio between thickness and length). The minimum limit thickness set by the vapor resistance threshold is:

$$t_{limit} = \left(\frac{\frac{L_{eff}}{k_s}a - \sqrt{\left(\frac{L_{eff}}{k_s}\right)^2 - 4\frac{r_w}{k_w}\left(\frac{1}{L_e}+\frac{1}{L_c}\right)\left(\frac{L_{eff}}{M_v r_v^3}\right)}}{2\frac{r_w}{k_w}\left(\frac{1}{L_e}+\frac{1}{L_c}\right)}\right)^{\frac{1}{2}} \tag{5}$$

where $a = 1 / (1 - r_{wl})$ and M_v is a constant that represents the properties of steam. This limit thickness is independent of the heat inlet; however, the capillary limit should be assessed simultaneously with this threshold, which should prevail over all moderate heat inputs. The properties of the steam that dictate the vapor resistance threshold are represented as a single factor that can be used as a number of merit for the choice of liquid in the design of ultra-thin heat pipes that operate at low temperature inputs:

$$M_v = \frac{h_{fg}^2 \rho_v P_v}{R \mu_v T_v^2} \tag{6}$$

which is not dependent of geometrical parameters.

3 2D Modeling approach

3.1 heat pipe configurations and associated equations

The standard configurations of flat heat pipes, which include wall, porous wick saturated with operating fluid, and vapor space are shown in figure 3 a, b: simple heat, multiple heat sources, underneath the heat source, and the radiator at the top of the heat pipe, multiple heat sources with symmetrical limit conditions. The basic assumptions are two-dimensional, constant material properties, constant saturation temperature and linear temperature profile across the structure of the wick.

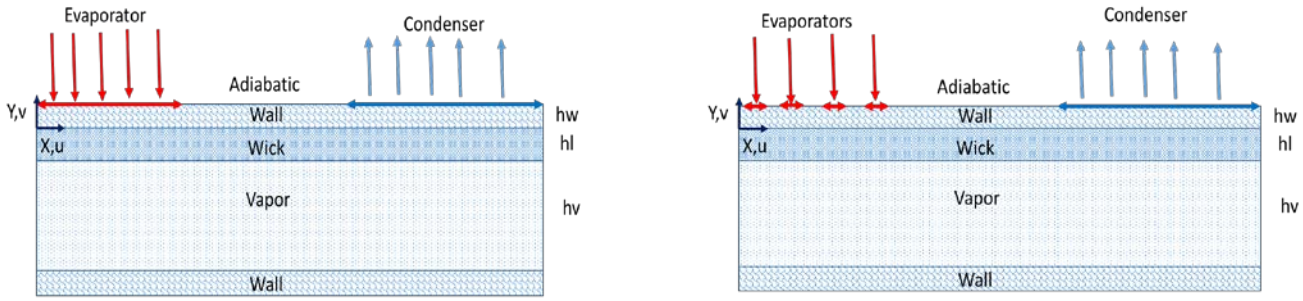

(a) Configuration I

(b) Configuration II

Figure 3 Flat heat pipe : different heating/cooling configurations: a) configuration I, single heat source and sink at the top; b) configuration II, multiple heat sources with sink at top.

- Conduction in wall[9]

The non-dimensional temperature, heat flux and coordinates can be defined as:

$$\vartheta = \frac{k_w}{q_e h_w}(T - T_{sat}) \tag{7}$$

$$\mathrm{X} = \frac{x}{l}; Y = \frac{y}{h_w}; H_w = \frac{h_w}{l}; H_l = \frac{h_l}{l}; L_e = \frac{l_e}{l}; L_c = \frac{l_c}{l}; \gamma = \frac{L_e}{L_c} \tag{8}$$

The two-dimensional dimensionless steady-regime heat conduction equation in the wall with constant thermal conductivity is :

$$\frac{\partial^2 \theta}{\partial X^2} + \frac{1}{H_w^2}\frac{\partial^2 \theta}{\partial Y^2} = 0 \tag{9}$$

For the condition on boundaries (X=0 and X=1) are

$$\frac{\partial \theta}{\partial X} = 0 \tag{10}$$

At the wick/wall interface (Y=0), the thermal boundary condition can be obtained assuming a linear temperature profile across the thin wick and a constant saturation temperature at the liquid-vapor interface. Then, the boundary condition are:

$$\frac{\partial \theta}{\partial Y} = \frac{k_{eff} H_w}{k_w H_l}\theta \tag{11}$$

The boundary condition at the outer wall (Y=0) are: constant heat fluxes in the evaporators and the condenser, with different locations on the heat pipe, and a heat flux null in the adiabatic sectionsb at the surface rest . That is：

$$\frac{\partial \theta}{\partial Y} = \begin{cases} 1 \ evaporator \\ 0 \ adiabatic \\ -\gamma \ condenser \end{cases} \tag{12}$$

The non-dimensional temperature for configurations I and II can be considered as an infinite Fourier series expansion:

$$\theta(X,Y) = \sum_{m=1}^{\infty} A_m(Y)\cos(m\pi X) \tag{13}$$

The non-dimensional input heat flux, location-dependant of heat sources and sinks, can be developed as follows:

$$\frac{\partial\theta}{\partial Y} = \sum_{m=1}^{\infty} B_m \cos(m\pi X) \tag{14}$$

where

$$B_m = \frac{2}{m\pi}\{\sin(m\pi L_{2e}) - \sin(m\pi L_{1e}) + \sin(m\pi L_{4e}) - \sin(m\pi L_{3e}) + \sin(m\pi L_{6e}) - \sin(m\pi L_{5e}) + \sin(m\pi L_{8e}) - \sin(m\pi L_{7e}) - \gamma[\sin(m\pi L_{2c}) - \sin(m\pi L_{1c})]\} \tag{15}$$

in which : $L_{1e}, L_{2e}, L_{3e}, L_{4e}, L_{5e}, L_{6e}, L_{7e}, L_{8e}, L_{1c}$ *and* L_{2c} express the heat sources and heat sink locations.

Substituting (13) and (14) into (9), (11) and (12), for the Am coefficient, leads to:

$$A_m(Y) = B_m \frac{\left(m\pi+\frac{k_{eff}}{k_w H_l}\right)\exp(m\pi H_w Y)+\left(m\pi-\frac{k_{eff}}{k_w H_l}\right)\exp(-m\pi H_w Y)}{m\pi H_w\left[\left(m\pi+\frac{k_{eff}}{k_w H_l}\right)\exp(m\pi H_w Y)-\left(m\pi-\frac{k_{eff}}{k_w H_l}\right)\exp(-m\pi H_w Y)\right]} \tag{16}$$

- Vapor flow

A parabolic velocity profile is used for vapor flow within the heat pipe. The velocity distribution is represented by a functional product in the x- and y-directions:

$$u_v(x,y) = -6U_v(x)\left[\left(\frac{h_l}{h_v}\right)^2 + \frac{h_l}{h_v} + \left(1+2\frac{h_l}{h_v}\right)\left(\frac{y}{h_v}\right) + \left(\frac{y}{h_v}\right)^2\right] \tag{17}$$

where $U_v(x)$ is the local mean velocity along the x-axis.

The continuity equation, for the two-dimensional incompressible vapor flow; can be integrated with respect to y, to determine $U_v(x)$

$$\int_{-(h_l+h_v)}^{-h_l}\left(\frac{\partial u_v}{\partial x}+\frac{\partial v_v}{\partial y}\right)dy = \int_{-(h_l+h_v)}^{-h_l}\frac{\partial u_v}{\partial x}dy + v_{v,I}(-h_l) - v_v(-(h_l+h_v)) \tag{18}$$

where $v_{v,I}$ is the vapor interfacial velocity. The heat flux, normal to the liquid-vapor interface; q_I , can be calculated from the conduction model, with the assumption of a linear temperature profile across the wick, getting :

$$v_{v,I}(-h_l) = \frac{q_I}{\rho_v h_{fg}} = q_e \frac{k_{eff}h_w}{\rho_v h_{fg} k_w h_l}\sum_{m=1}^{\infty} A_m(0)\cos\left(\frac{m\pi x}{l}\right) \tag{19}$$

$$v_v(-(h_l+h_v) = 0 \tag{20}$$

Integrating Eq. (20), with respect to x, and using the boundary condition at the beginning of the evaporator - $u_v = 0$ −, results in the following expression for $U_v(x)$:

$$U_v(x) = q_e \frac{k_{eff}h_w}{\rho_v h_{fg} k_w h_l}\sum_{m=1}^{\infty}\left(\frac{l}{m\pi}\right)A_m(0)\sin\left(\frac{m\pi x}{l}\right) \tag{21}$$

Therefore, the quasi-two-dimensional velocity profile can be written:

$$u_v(x,y) = -6q_e \frac{k_{eff}h_w}{\rho_v h_{fg} k_w h_l} \sum_{m=1}^{\infty} \left(\frac{l}{m\pi}\right) A_m(0) \sin\left(\frac{m\pi x}{l}\right) \times \left[\left(\frac{h_l}{h_v}\right)^2 + \frac{h_l}{h_v} + \left(1 + 2\frac{h_l}{h_v}\right)\left(\frac{y}{h_v}\right) + \left(\frac{y}{h_v}\right)^2\right] \quad (22)$$

The boundary layer of the x-momentum equation, for steady-state incompressible laminar vapor flow, can be integrated , obtaining the vapor pressure distribution:

$$\rho_v \int_0^x \int_{-(h_l+h_v)}^{-h_l} \frac{\partial (u_v)^2}{\partial x} dxdy + \rho_v \int_0^x \int_{-(h_l+h_v)}^{-h_l} \frac{\partial (u_v v_v)}{\partial y} dxdy = \int_0^x \int_{-(h_l+h_v)}^{-h_l} -\frac{\partial p_v}{\partial x} dxdy + \mu_v \int_0^x \int_{-(h_l+h_v)}^{-h_l} \frac{\partial^2 (u_v)}{\partial y^2} dxdy \quad (23)$$

Assuming a constant vapor pressure at each cross-section, and considering the boundary conditions at the front of the evaporator, $u_v = 0$ and $p_v = p_{ref}$, yields to:

$$p_v = p_{ref} + q_e \frac{k_{eff}h_w}{\rho_v h_{fg} k_w h_l h_v^3} \sum_{m=1}^{\infty} A_m(0) \left[\cos\left(\frac{m\pi x}{l}\right) - 1\right] + 18\rho_v U_v^2 \left[\frac{1}{5}\left(\frac{h_l}{h_v}\right)^5 + \frac{1}{30}\right] \quad (24)$$

where U_v is obtained from (21).

The temperature drop in the vapor can be linked to the pressure drop in the vapor area , considering the Clausius-Clapeyron equation, and using the ideal gas law:

$$T_v = \frac{1}{\frac{1}{T_{ref}} - \frac{R}{h_{fg}} \log\left(\frac{p_v}{p_{ref}}\right)} \quad (25)$$

where R is the ideal gas constant, h_{fg} is the latent heat, and p_v is the pressure drop obtained from (24).

- Liquid flow

The continuity equation, for an incompressible liquid flow, can be integrated with respect to y, thus obtainingthe liquid axial velocity $u_l(x)$:

$$\int_{-h_l}^{0} \left(\frac{\partial u_v}{\partial x} + \frac{\partial v_v}{\partial y}\right) dy = -v_{l,I}(-h_l) - h_l \frac{du_l}{dx} \quad (26)$$

where $v_{l,I}$ represents the interfacial velocity (normal to the liquid vapor interface) for the liquid and is related to the vapor interfacial velocity by:

$$\rho_l v_{l,I} = \rho_v v_{v,I} \quad (27)$$

The axial liquid velocity can be calculated by integrating (26) with respect to x, using the velocity boundary condition at the beginning of the evaporator (x = 0), $u_l = 0$:

$$u_l(x) = q_e \frac{k_{eff}h_w}{\rho_v h_{fg} k_w h_l^2} \sum_{m=1}^{\infty} \left(\frac{l}{m\pi}\right) A_m(0) \sin\left(\frac{m\pi x}{l}\right) \quad (28)$$

The one-dimensional steady-regime momentum conservation, for incompressible liquid flow in the wick, can be expressed by a Darcy's law, assuming negligible the inertial effects compared to viscous losses, as:

$$\frac{dp_l}{dx} = -\frac{\mu_l u_l}{K} \quad (29)$$

in which the permeability K is calculated for a mesh screen as:

$$K = \frac{d^2 \varphi^3}{122(1-\varphi)^2} \quad (30)$$

$$\varphi \approx 1 - \frac{1.05\pi Nd}{4} \tag{31}$$

The liquid pressure is derived by integrating (30) and utilizing the pressure boundary condition at the end of the condenser (x=l), $p_l = p_v$:

$$p_l = q_e \frac{\mu_l k_{eff} h_w}{\rho_l h_{fg} k_w K h_l^2} \sum_{m=1}^{\infty} (\frac{l}{m\pi})^2 A_m(0) \left[\cos\left(\frac{m\pi x}{l}\right) - \cos(m\pi)\right] + p_{ref} + q_e \frac{12\mu_v k_{eff} h_w}{\rho_v h_{fg} k_w h_v^3 h_l} \sum_{m=1}^{\infty} (\frac{l}{m\pi})^2 A_m(0)[\cos(m\pi) - 1] \tag{32}$$

We give also capillary pressure

$$p_{cap} = p_v - p_l \tag{33}$$

FEM verification results

The schematic diagram of the simulated geometries is shown in the figure 4.

The properties of the working fluid, copper and porous wick materials, used in the vapor core chamber simulations, are shown in table1. Vapor properties are shown for a 40degC temperature.

Table1 Working fluid properties; porous wick and copper materials used in the simulations of the heat pipe

PROPERTY	VALUE
Copper density(ρ_{wall})	8978kg/m3
Water liquid density(ρ_{water})	992.3kg/m3
Water vapor density(ρ_v)	0.05122kg/m3
Copper thermal conductivity(k_{wall})	400W/mK
Wick effective thermal conductivity(k_{wick})	1.3W/mK
Water vapor thermal conductivity(k_v)	0.05W/mK
Copper specific heat capacity(C_p)	381 J/kgK
Water liquid specific heat capacity(C_p)	4182 J/kgK
Water vapor specific heat capacity(C_p)	1889 J/kgK
Water liquid viscosity(μ_l)	0.00065 Pa*s
Water vapor viscosity(μ_v)	0.0000096 Pa*s
Enthalpy of vaporization(h_{fg})	2473 kJ/kg
Specific gas constant(R_const)	8.3145 J/molK
Water vapor mean molar mass(M_n)	0.018015 kg/mol
Wick porosity(φ)	0.5
Wick permeability(K)	1*10-11 m2

Therefore, the temperature fields predicted by the modeling approaches are shown in Figure 4. (a) shows the temperature profile comparisons along the x directions, of 50W heat source, between COMSOL and publication Maziar Agnvami [14] ; the error between them, while Figure 4(b) shows the COMSOL simulated temperature profile with 30W, 40W and 50W heat source. The temperature profile has a maximum temperature, at the evaporation side, in the top surface and a minimum temperature at the condenser side. Plots reveal a very good accuracy match between COMSOL and the theoretical solution. The maximum error is about 6% for configuration I and 0.075% for configuration II. From Figure 4 (b) & (d), we observe that, by adding 10W at the heat source, the temperature gains about 3K for configuration I and 4K for configuration II.

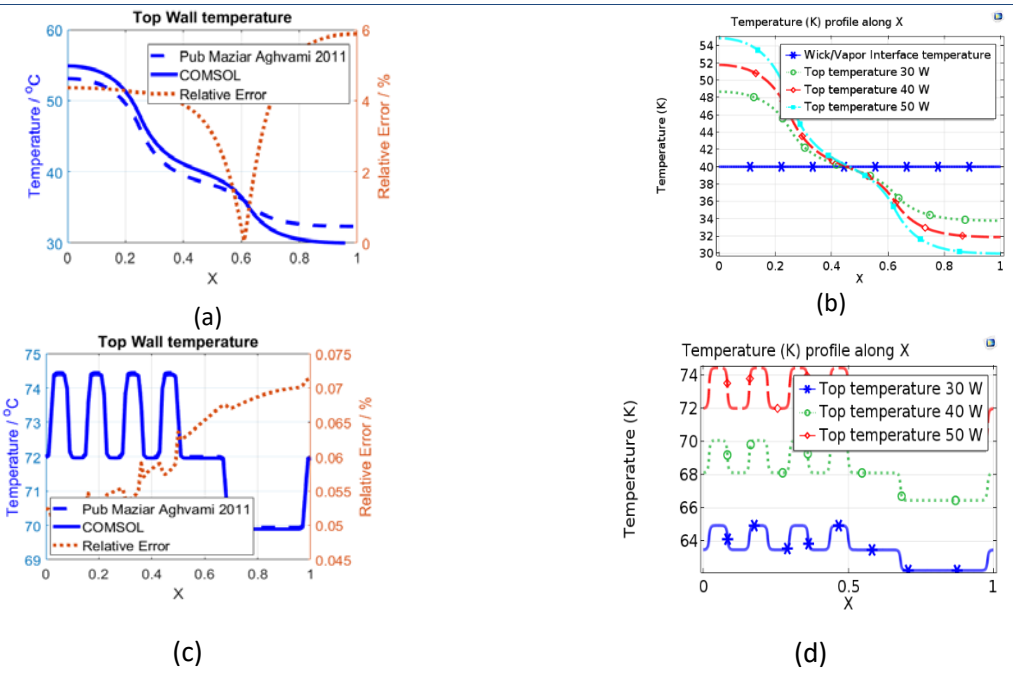

Figure 4 Temperature profile (a) comparison between COMSOL and pub with 50W heat source [14] in Matlab configuration I (b) parametrization of power in COMSOL configuration I (c) comparison between COMSOL and pub with 50W heat source [14] in Matlab configuration II (d) parametrization of power in COMSOL configuration II

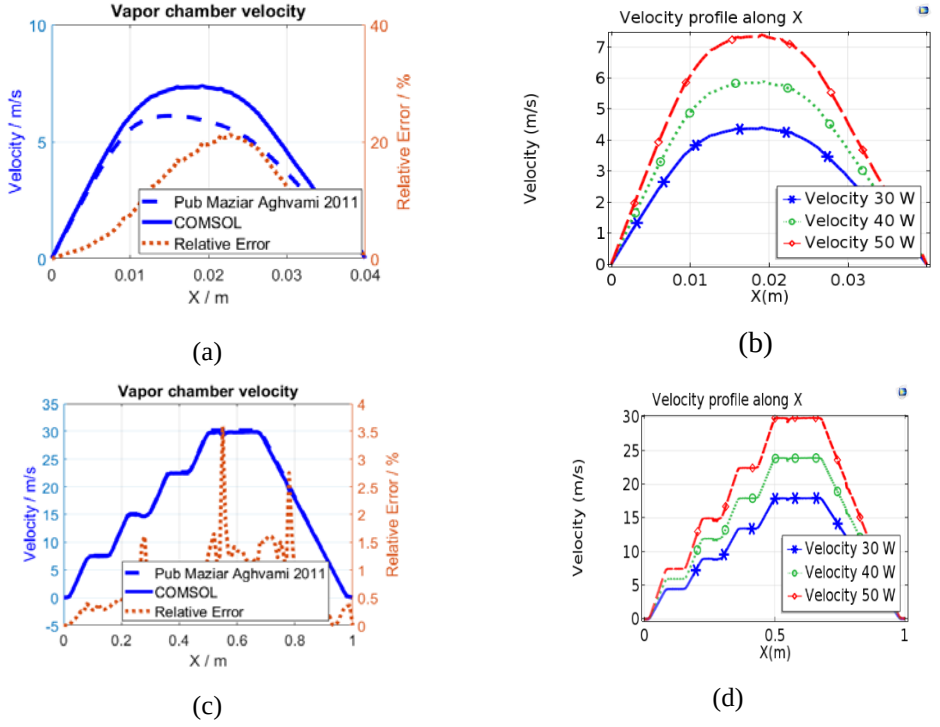

Figure 5 velocities at the center of the vapor chamber (a) comparison between COMSOL and pub with 50W heat source [14] in Matlab configuration I (b) parametrization of power in COMSOL configuration I (c) comparison between COMSOL and pub with 50W heat source [14] in Matlab configuration II (d) parametrization of power in COMSOL configuration II.

The Figure 5 compares the velocities at the center of vapor chamber.

As we can see in the figure 5, the vapor has a maximum velocity at the vapor core center and reduces to 0 when it attaches the wall. And for the COMSOL model, the maximum velocity is about 7m/s, that is almost the same for the velocities of paper[14]. For configuration I, there is about 20% difference between analytical solution and COMSOL; especially for the analytical solution, the velocity of configuration I has a non-symmetry form. But for configuration II, the difference in velocity is less than 4%. And by increasing 10W of the heat source, the velocity gains about 1.5m/s for configuration I and 6m/s for configuration II.

Finally, the most important part of the heat pipe is the capillary pressure at the vapor/wick interface. Fig 6 shows the capillary pressure at the wick/vapor interface On the steam, the water is evaporated and the steam has a maximum pressure on the surface; but next to the condenser , condensates water and creates fluid in the water, so the opposite process along with condensation and mass flow in relation to the evaporator, so that the water evaporates to the ground at condensation. It is much slower than the steam core. Figure 6 shows the COMSOL simulation and publication configuration [14], with a capillary difference of up to 20% pressure. But in the configuration II capillary pressure is almost identical. And it's less than the defect 0.5%.

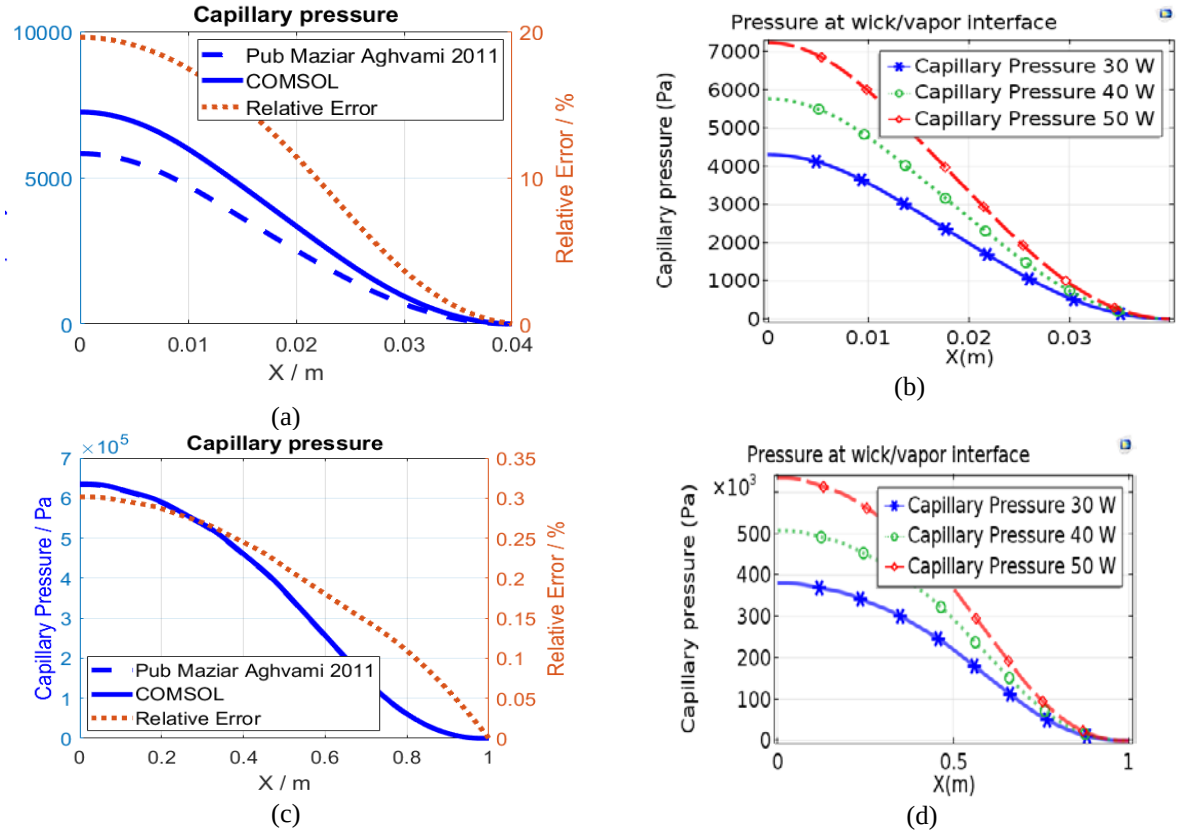

Figure 6 Capillary pressure at the wick/vapor interface (a) comparison between COMSOL and pub with 50W heat source [14] in Matlab configuration I (b) parametrization of power in COMSOL configuration I (c) comparison between COMSOL and pub with 50W heat source [14] configuration II (d) parametrization of power in COMSOL in Matlab configuration II.

In the vapor chamber operation, a steady state model is developed, which allows for multiple, arbitrarily shaped, heat inputs on the evaporator-side face; model offers 2D temperature, pressure and speed ranges in the steam chamber, depending on the size of the camera, liquid and steam flow and material properties hypotheses. The governing mass, power, momentum and energy equations are set on the wall, wick and steam core domains. The model is compared to the numerical model [14].

3.1 Standalone chip

The first step consists to create a numerical model representing a standalone system [22]as shown in Figure 7. These ICs do not constitute a set of simple layers, but many small components (cf., electrical communication) that would be not easy to discretize. For he sake of practicability, these components are homogenized by substances in their environment, using the method proposed by Crécy [23]. Flat and simple heat conductors are independently referred to a representing thermal behavior in these domains. Micro heat pipe are in the Si die to the Si molding junction. The geometry of the model containing homogeneous regions is shown in Figure 8. Table 2 summarizes the thermal transitions and measurements used. The thermal conductivity is estimated by force law on the basis of empirical results [24].

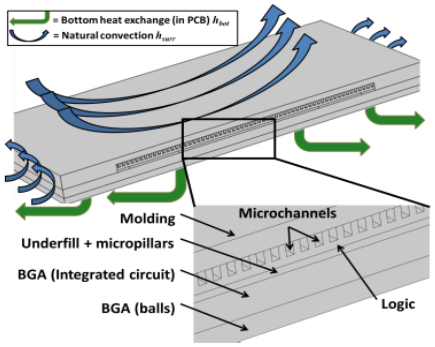

Figure 7 Simulated standalone chip

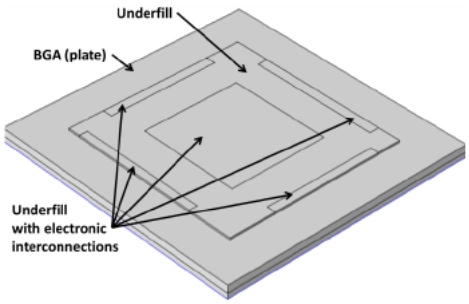

Figure 8 Simulated standalone chip showing the layer below logic die

Table 2 – Chip layer dimensions and thermal conductivities

Layer	Thermal Conductivity (W/m-K)		Thickness (µm)	Sides (mm)
-	Planar	Normal	-	-
Molding	0.88		200 (above logic)	12 X 12
Si die	$161\,952*T^{-1.225}$		200	8.5 X 8.5
Underfill (polymer)	1.5		70	8.5 X 8.5
*Underfill (polymer+pillars)	1.9	3.5	70	
BGA (substrate)	92	0.6	288	12 X 12
BGA (balls array)	0.7	8	210	

T: Temperature [K]
*: Homogenized zone

The boundary conditions surrounding the chip are natural convection,with a convection coefficient estimated to h_{surr}=10 W/m²K [22]. The bottom of the model is normally linked to a Printed Circuit Board

(PCB), which allows important lateral heat spreading, with an equivalent convection coefficient estimated to h_{bot}=570 W/m²K [22]

3.1.1 Heat management

The heating power is distributed into the 8-core of 360X490 mm² to represent the test chip, as seen in Fig. 9. With a 2W per core, a total of 16 W needs to be removed. For correct operation, the chip temperature, , should be below 125 degrees. Ambient temperature and inlet temperature are set at 40 ° C, which is recommended for indoor air.

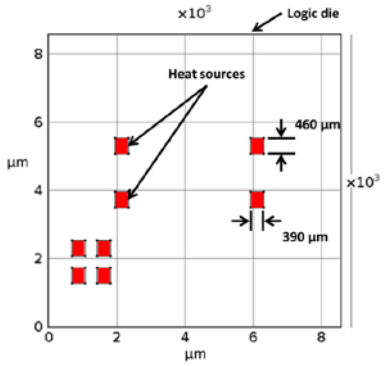

Figure 9 Heat sources layout, on the standalone chip

4 Results And Discussion

4.1 Uncooled chip

The reference case is simulated without micro-heating pipes. In this case, chip is exclusively cooled by expansion during the BGA and normal convection. In Figure 10, the reference case is simulated without micro-heating pipes. In our case, the piece is exclusively cooled by expansion during the BGA and normal convection. I expect 10 maximum temperatures above the maximum allowed temperature of 125 ° C, which indicates the need for cooling. The maximum temperature is above the maximum allowed one: 125 ° C, which clearly shows the need for cooling solution.

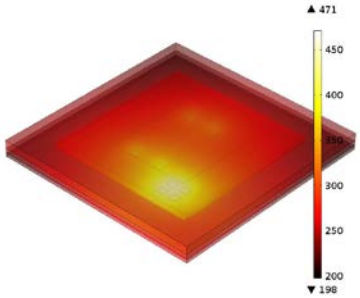

Figure 10 Chip: simulation without microchannels; extracted heat, only by natural convection and PCB heat spreading

4.1.1 Micro-heat pipe integration with standalone chip

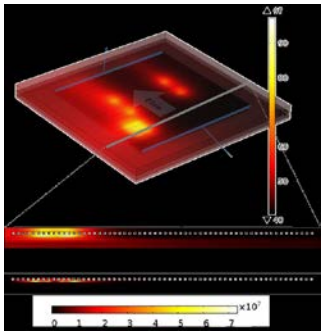

Figure 11 Micro-heat pipe- simulation- dissipating 16W in a flip-chip with xx 85mm long and 200um thick

4.1.2 Standalone chip application

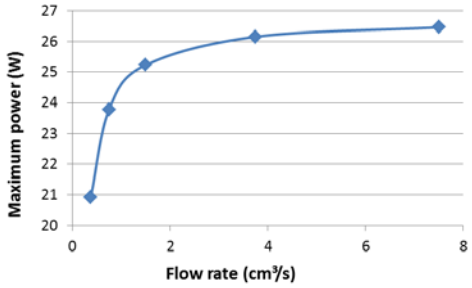

Figure 12 Maximum power admissible fot reaching a maximum temperature of 125 °C, according to heat pipe length-to-thick ratio.

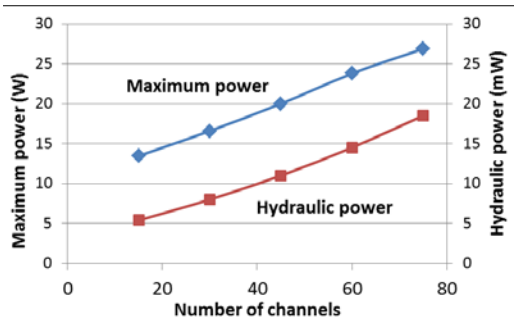

Figure 13 Maximum possible power for micro-heat pipe; simulation with different porous thermal conductivities

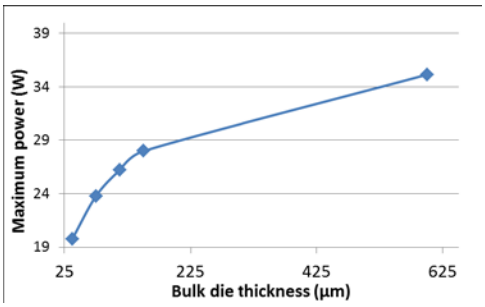

Figure 14 Maximum power admissible versus die bulk thickness

5 Conclusion

Analytical and numerical modeling, and experimental simulations of the heat pipes significantly facilitated a much better understanding of the various physical phenomena found in the heat pipes and the development of computer and experimental methods.

FEM models (COMSOL Multiphysics) are very accurate in the 2D and 3D simulation of the heat pipe. Exact limit conditions can be found in the previous section; consider the pressure factor in the calculation and specifically extract the capillary pressure from wick layer's capillary. In the course of future work, the

streamlining of the evaporated material needs to be changed to temperature-dependent parameters and due to the simplification requirements; the quantitative analysis of the model error is performed in a range of operating conditions.

This model changes to a 3D model and uses multiple thermal input boundary conditions to simulate the behavior of the steam chamber to demonstrate its ability to solve the 3D thermal response to complex boundary conditions expected in real applications. Before some true applications are introduced, some transfer mechanisms will be included in the model. These include the effect of external boundary conditions on the interface mass flow profile, the vapor convection, and the flux of the interface mass in the adiabatic phase with a 2-D drive. However, these additional mechanisms should be taken into account in detailed numerical models for the application-oriented design and optimization of ultrathin heat pipes. This study highlights the relative importance of the three types of resistances in the microfluidic chip cooling and that conventional thinking is challenging if we take real module configurations into account.

REFERENCES

[1] D. Milojevic, H. Oprins, J. Ryckaert, P. Marchal, and G. Van Der Plas, "DRAM-on-logic stack - Calibrated thermal and mechanical models integrated into PathFinding flow," *Proc. Cust. Integr. Circuits Conf.*, pp. 5–8, 2011.

[2] C. Torregiani, H. Oprins, B. Vandevelde, E. Beyne, and I. De Wolf, "Compact thermal modeling of hot spots in advanced 3D-stacked ICs," *Proc. Electron. Packag. Technol. Conf. EPTC*, no. 1, pp. 131–136, 2009.

[3] L. Lin, R. Ponnappan, and J. Leland, "High performance miniature heat pipe," *Int. J. Heat Mass Transf.*, vol. 45, no. 15, pp. 3131–3142, 2002.

[4] W. Huang, S. Ghosh, S. Velusamy, K. Sankaranarayanan, K. Skadron, and M. R. Stan, "HotSpot: A compact thermal modeling methodology for early-stage VLSI design," *IEEE Trans. Very Large Scale Integr. Syst.*, vol. 14, no. 5, pp. 501–513, 2006.

[5] W. S. Zhao, J. Zheng, S. Chen, X. Wang, and G. Wang, "Transient Analysis of Through-Silicon Vias in Floating Silicon Substrate," *IEEE Trans. Electromagn. Compat.*, vol. 59, no. 1, pp. 207–216, 2017.

[6] U. Vadakkan, S. V. Garimella, and J. Y. Murthy, "Transport in Flat Heat Pipes at High Heat Fluxes From Multiple Discrete Sources," *J. Heat Transfer*, vol. 126, no. 3, p. 347, 2004.

[7] Y. Luo, B. Yu, X. Wang, and C. Li, "A novel flat micro heat pipe with a patterned glass cover," *IEEE Trans. Components, Packag. Manuf. Technol.*, vol. 6, no. 7, pp. 1053–1057, 2016.

[8] J. P. Longtin, B. Badran, and F. M. Gerner, "A One-Dimensional Model of a Micro Heat Pipe During Steady-State Operation," vol. 1, no. AUGUST 1994, 2014.

[9] S. Lips and F. Lefèvre, "A general analytical model for the design of conventional heat pipes," *Int. J. Heat Mass Transf.*, vol. 72, pp. 288–298, 2014.

[10] L. Lin, R. Ponnappan, and J. Leland, "High performance miniature heat pipe," *Int. J. Heat Mass Transf.*, vol. 45, no. 15, pp. 3131–3142, 2002.

[11] H. Li, Y. Tang, Y. Jin, B. Li, and T. Zou, "Experimental Analysis and FEM Simulation of Antigravity Loop-Shaped Heat Pipe for Radio Remote Unit," pp. 1–9, 2017.

[12] R. Hopkins, A. Faghri, and D. Khrustalev, "Flat Miniature Heat Pipes With Micro Capillary Grooves," *J. Heat Transfer*, vol. 121, no. 1, pp. 102–109, 1999.

[13] Y. Ma. and C. Gontrand, "Power, Thermal, Noise and Signal Integrity Issues on substrate/Interconnects entanglement" *CRC press*, 2018.

[14] M. Aghvami and A. Faghri, "Analysis of flat heat pipes with various heating and cooling configurations," *Appl. Therm. Eng.*, vol. 31, no. 14–15, pp. 2645–2655, 2011.

[15] Z. J. Zuo and A. Faghri, "A network thermodynamic analysis of the heat pipe," *Int. J. Heat Mass Transf.*, vol. 41, no. 11, pp. 1473–1484, 1998.

[16] U. Vadakkan, J. Y. Murthy, and S. V Garimella, "Transient Analysis of Flat Heat Pipes," pp. 1–11, 2017.

[17] G. Patankar, J. A. Weibel, and S. V Garimella, "A Time-Stepping Analytical Model for 3D Transient Vapor Chamber Transport," 2017.

[18] R. S. Prasher, "A Simplified Conduction Based Modeling Scheme for Design Sensitivity Study of Thermal Solution Utilizing Heat Pipe and Vapor Chamber Technology," *J. Electron. Packag.*, vol. 125, no. 3, p. 378, 2003.

[19] C. Byon, K. Choo, and S. J. Kim, "Experimental and analytical study on chip hot spot temperature," *Int. J. Heat Mass Transf.*, vol. 54, no. 9–10, pp. 2066–2072, 2011.

[20] L-M. Collin V. Fiori P. Coudrain S. L. Lhostis S. Chéramy J-P Colonna B. Mathieu A. Souifi, L. G. Fréchette "Microchannel design study for 3D microelectronics cooling using a hybrid analytical and finite element method ", Proceedings of the ASME 2015, 13th International Conference on Nanochannels, Microchannels, and Minichannels, July 6-9, 2015, San Francisco, California, US.

[21] Y. Yashwanth, J. A. Weibel, and S. V Garimella, "Performance-Governing Transport Mechanisms for Heat Pipes at Ultra-thin Form Factors Performance-Governing Transport Mechanisms for Heat Pipes at Ultra-Thin Form Factors," vol. 5, no. 11, pp. 1618–1627, 2015.

[22] R. Prieto et al., "Thermal measurements on flip-chipped system-on-chip packages with heat spreader integration," *SEMI-THERM*, pp. 221–227, 2015.

[23] F. de Crécy, "A simple and approximate analytical model for the estimation of the thermal resistances in 3D stacks of integrated circuits," *Int. Work. Therm. Investig. ICs Syst.*, no. September, pp. 1–6, 2012.

[24] Hull R.;, *Properties of Crystalline Silicon*. London - United Kingdom, 1999.

SOCIETY FOR SCIENCE AND EDUCATION
UNITED KINGDOM

TNC TRANSACTIONS ON NETWORKS AND COMMUNICATIONS

VOLUME 7, NO. 6
ISSN: 2054 -7420

Study of PH and Electrical Conductivity in Soil of Barnala District (Punjab, India): Deleterious Effects on Human Lives

Dr. Kamalpreet Kaur
Department of Chemistry, Assistant Professor, Guru Gobind Singh Khalsa College Bhagta Bhai Ka Bathinda, Punjab(INDIA)
k.kdhaliwal.dhaliwal@gmail.com

ABSTRACT

The purpose of this study was to determine the pH and electrical conductivity in soil of different villages of barnala district (Punjab,India) and their harmful effects on human health. Samples of soil were collected from agricultural fields of four different villages of barnala region such as Rure ke kalan, Gunas, Handiaya and cheema from five different layers(0-10 cm; 10-20 cm; 20-30 cm; 30-40 cm and 40-50 cm depth).There are three industrial sites in barnala district and these four villages are located near to these industial sites. In this study, adverse effect of different industries on fields of these four villages were investigated. Handiaya village has high values of pH and electrical conductivity while Gunas and Cheema villages have lowest value of electrical conductivity and pH respectively. when textile effluent reaches the soil or underground water it causes bad effect on human health such as people may suffer from alkalosis which is due to high pH and can lead to arrhythmia which means irregular heartbeat. Alkalosis can induce a coma, it may cause seizures and malfunctioning of kidneys. Due to large value of Electrical conductivity activity of soil micro-organism declines so, the important microbial processes, such as nitrogen cycling, production of nitrous and other N oxide gases, respiration, and decomposition; populations of plant-parasitic nematodes can increase; and increased nitrogen losses.

Keywords- Soil contamination, Physico-chemical parameters, pH, electrical conductivity

1 Introduction

Measuring of pH and electrical conductivity (EC) parameters will provide valuable information for assessing soil condition for plant growth, nutrient cycling and biological activity. Soil pH measurement is useful because it is a predictor of various chemical activities within the soil. As such, it is also a useful tool in making management decisions concerning the type of plants suitable for location, the possible need to modify soil pH (either up or down), and a rough indicator of the plant availability of nutrients in the soil. The Electrical Conductivity (EC) of a solution is a measure of the ability of the solution to conduct electricity. The EC is reported in either millimhos per centimeter or the equivalent decisiemens per meter. When ions (salts) are present, the EC of the solution increases.

If no salts are present, then the electrical conductivity is low indicating that the solution does not conduct electricity well. The EC indicates the presence or absence of salts, but does not indicate which salts might be present. For example, the EC of a soil sample might be considered relatively high. Frequent use of

DOI: 10.14738/tnc.76.7585
Publication Date: 28th Dec 2019
URL: http://dx.doi.org/10.14738/tnc.76.7585

irrigation water will directly influence the salts in the soil profile. Salts are influenced by factors such as rainfall content and timing, internal soil drainage, and irrigation practices. Usually, rainfall contains low amounts of salts and acts to dilute salts that are present in the soil. If the rainfall is of sufficient volume or duration, and the soil has internal drainage, the added rainfall is enough to leach salts from the soil. During drying conditions, water is lost from the soil due to evaporation, and salts are effectively concentrated. If irrigation water contains appreciable salts, then intensive management is required to produce healthy plants.

2 Material and methods

Barnala(Punjab,India) is situated between 30° 23' North and 75° 33' East. It has a mean elevation of 227 metres (745 feet).It is located on the Bathinda-chandigarh highway (no-7) and the Jalander-Rewari national highway (no-71),The Sirsa-Ludhiana state highway (no-13) are passes through it. It is 65 km from Bathinda and 85 km from Ludhiana.According to 2011 census, the total population of Barnala district is 595527.It was 526931 in 2001.

The sampling time was between 4:30 to 5:30 on 9th November 2016.Plastic polythene bags were used to collect soil samples

MAP OF BARNALA DISTRICT

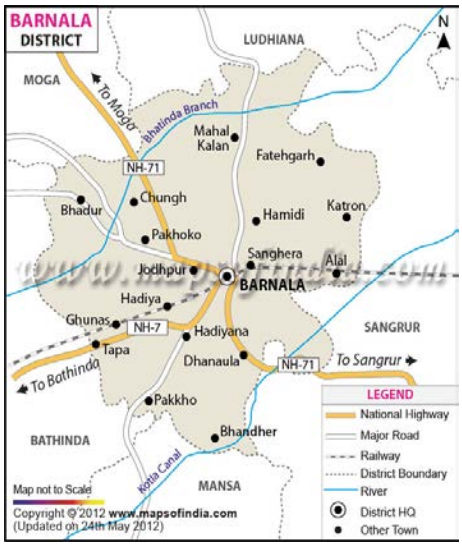

3 Sample collection

Soil samples were collected from agricultural fields of four villages such as Rure ke kalan, Gunas, Handiaya and cheema which are present near to industrial sites. These four villages are located in Barnala district (Punjab, India).Soil samples were collected from five sampling depths 0-15 cm, 15-30 cm, 30-45 cm, 45-60 cm and 60-75 cm. . Five sub-samples were taken within an area of 100 m² from each sampling location. About 1 kg weight of each sub- sample were collected.

Determination of pH-

It is determined by pH meter.

Principle- The pH is measured electrometrically by means of an electrode assembly consisting of one glass electrode and one calomel reference electrode

with a saturated potassium chloride.

Potassium chloride is used for the salt bridge because of the fact that the transfer of K+ and Cl^- ions takes place at the rate in true solution. The pH determination by this method is based on the assumption that the potential recorded is totally due to the potential difference across the glass membrane brought about the difference in H+ ion activity, between solution inside and outside the glass electrode. The outside solution is hydrochloric acid.

Interference-Several factors are known to affect the pH- value of a particular sample. Prominent amongst these are soil-water ratio, Soluble salt concentration, CO2 pressure, exchangeable actions and temperature. With the dilution of soil suspension, its pH increases. Increases in salt concentration in general decreases pH, In alkaline soils, the pH is influenced by exchangeable cations.With increase in temperature, pH decrease. The effect of temperature is controlled with instrument having temperature compensation system.

Apparatus- pH meter that is a high impedance voltmeter calibrated in terms of pH, balance sensitive to 0.001 gm, general laboratory glass wares.

Reagents –

1 Buffer solutions- Of pH values namely 4.00,7.00 and 9.20
2 Buffer solution pH 4.0 (at 25°C)-Dissolve 5.106 gm of potassium hydrogen phthalate in distilled water and dilute to 500ml with distilled water.
3 Buffer solution pH 7.0 (at 25°C)- Dissolve 1.678 gram sodium dihydrogen phosphate in distilled water and make up to 500 ml with distilled water.
4 Buffer solution pH 9.2 (at 25°C)- Dissolve 9.54 gm of sodium tetraborate (borax) in distilled water and dilute it 500 ml. Pure chemical CRM/ AR grade shall be used. Buffer solutions can also be prepared from (available commercially) buffer tablets or powder. Standard pH buffer solutions(CRM) are preferred.

Procedure-

A) preparation of soil sample-

1. 1.The sample received from the field shall be prepared.All aggregations of soil particles shall be broken down , thoroughly mixed and received on a suitable sieve(2mm).
2. Take 30 gm of the soil from the sample as prepared above in a 100ml beaker, add 75ml distilled water. Stir the suspension for few minutes. Cover the beaker with which glass and allow to stand for one hour, with occasional stirring. It shall be again stirred well immediately before testing.

B) Operation-

1. Calibration of pH meter- The pH meter shall be calibrated by means of standard buffers. Attach pH electrode with pH meter set the temperature compensating knob and confirm that electrode is completely filled with standard KCl solution. Allow pH meter to warm up for 15 minutes.The

instrument is then set with standard buffer solution of value pH-7.0 shall be cross checked with another standard pH buffer solution pH 9.2 or 4.0

2. Testing of sample- Remove the electrode from the standard buffer solution, rinse it with distilled water and wipe/ dry with tissue paper. And then immerse it in the soil water suspension (1:2.5) ratio. Record pH meter reading. Two or three reading of the pH shall be taken with brief stirrings in between each reading. The readings should agree with ±0.05 pH units and should reach a constant value in about one minute. After final pH reading, remove the electrode from the ash suspension ,wash with distilled water , wipe it with tissue paper and check once again the calibration of pH- meter with one of the standard buffer solution. If the instrument is out of adjustment by more than 0.05 pH unit, it shall be set to the correct adjustment till consistent readings are obtained.

Determination of specific electrical conductivity-

Principle-Air dried soil is extracted with water at 25°C at an extraction ratio of 1:2 (m/v) to dissolve the electrolyte EC of the suspension extract is measured temperature affects conductivity as such increase in temperature promotes dissection with a consequent rise in conductivity, hence it is conveniently reported at 25°C.

Interference- Temperature affects electrical conductivity,which vary by absent 2% per day we Celsius. High silica contents give relatively low value of electrical conductivity.

Apparatus/ instrument- Conductivity meter giving direct reading of conductance and having automatic temperature compensation built in the instrument. Conductivity Cell, analytic balance,Thermometer, Shaking machine, Beakers.

Reagents- Potassium chloride solution (0.01M)-Dissolve 0.7456 gm of of AR/CRM grade KCl dried at 80°C for 1 hour in water and dilute it to 1000 ml.The specific electrical conductivity of this ash is 1413µ mhos/cm at 25°C.

Procedure-

A) Preparation of sample- All the aggregation of air derived particles shall be broken down, thoroughly mixed and sieved on a 2mm sieve. The electrical conductivity of soil is commonly measured in saturated extract and 1:2 soil water extract.

Preparation of soil saturation extract-

1. Take 100 gm of air dried soil sample sieved through 450 micron IS sieve in a beaker. Add distilled water slowly and stir the contents with spatula adding more water if required, till it attains the saturation stage.
2. Allow the beaker to stand as such for 2-3 hour and check the saturation stage (and for coarse texture soil, 4 hours time is sufficient). At saturation , soil paste glistens as it reflects light, flows slightly when the beaker is tipped and slides freely and cleanly off the spatula .There should be no free flowing water on the soil surface.
3. Transfer the saturation soil paste to a Buchner funnel with whatman No. 40 filter paper and the Buchner funnel attach to vacuum pump. Collect the extract. If the extract is turbid, re-filter the extract.

4. Transfer carefully all the aliquot of extract in a 100 ml volumetric flask and make up to the mark with distilled water. Add 4-5 drops of 0.1% sodium hexametaphosphate.To prevent the precipitation of calcium carbonate upto standing. (there may be increase in Na concentration due to addition of sodium hexametaphosphate but less than 0.5 ppm).

B) Weigh 20 gram of the ash and transfer it to 100 ml beaker.Add 40 ml of distilled water. Shake the soil water suspension for 30 minutes with a glass rod.

C) Measurement of electrical conductivity of the suspension-

1. warm up the instrument for 15 minutes calibrate the instrument with standard KCl (0.01M) solutions and adjust the all content of electrical conductivity meter.In case where correction for all content and temperature factor is not provided in instrument compare the cell constant as follows.

   K=Xs / Xm

   Where,

   K= cell constant

   Xs = specific conductivity of standard KCl (0.01M)

   Solution ,known value i.e 1413µmhos/cm at 25°C.

   Xm= Observed EC value of the standard KCl solution.

2. Adjust the all constant of the electrical conductivity meter and the temperature. Take the test soil suspension sample in a beaker.Record the exact temperature of the sample rinse the conductivity cell with the distilled water and increase it in soil sample take reading of conductivity.

D) Calculations-

Electrical conductivity (EC) µmhos/cm at 25°C=EC of suspension in µmhos/cm at 25°C × Cell constant (K) at 25°C.

4 Results and discussion-

Values of pH and electrical conductivity of soil water ratio-1:2 are given in tables

Table 1 of Site A

Depth of Soil (cm)	pH	EC
0-15	8.2	450
15-30	8.5	457
30-45	8.7	460
45-60	8.8	466
60-75	8.9	470
Mean ± S.D	8.62 ±0.277	460.6±7.79

Table 2 of Site B

Depth of Soil (cm)	pH	EC
0-15	8.1	202
15-30	8.3	209
30-45	8.6	212
45-60	8.8	217
60-75	9.0	220
Mean ± S.D	8.56 ± 0.364	212±7.03

Table 3 of Site C

Depth of Soil (cm)	pH	EC
0-15	8.0	1206
15-30	8.2	1213
30-45	8.4	1221
45-60	8.6	1227
60-75	8.8	1230
Mean ± S.D	8.4 ± 0.316	1219.4±9.91

Table 4 of Site D

Depth of Soil (cm)	pH	EC
0-15	8.0	503
15-30	8.1	508
30-45	8.2	516
45-60	8.4	522
60-75	8.5	530
Mean ± S.D	8.24 ± 0.207	515.8±10.77

With the increase of depth of soil values of pH and EC increases. These four sites corresponds to the four villages of barnala district. Site C has maximum value of pH and EC.

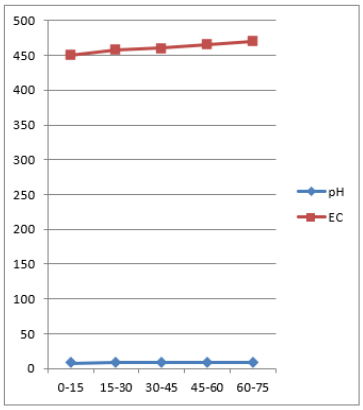

Graph of Site A

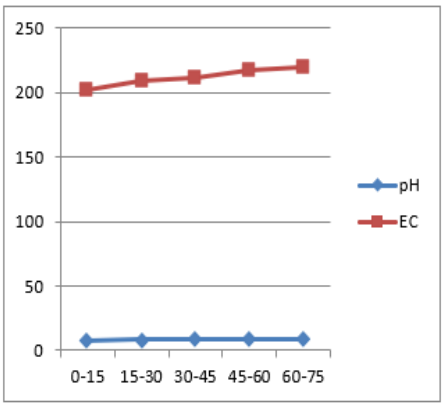

Graph of Site B

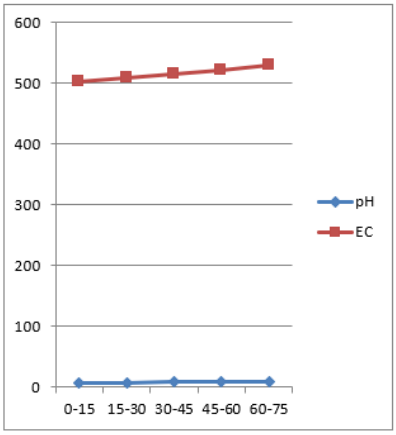

Graph of Site C

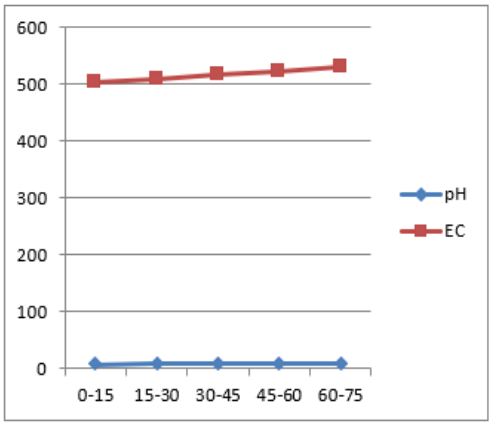

Graph of Site D

Five depths of soil are considered such as 0-15 cm, 15-30 cm, 30-45 cm, 45-60 cm, 60-75 cm in four different villages or sites.

5 Statistical analysis

The data obtained subjected to statistical analysis. In statistical analysis, a correlation developed between pH and Electrical conductivity by using KARL PEARSONS Coefficient of correlation.

Calculation of KARL PEARSON's Coefficient of correlation

Correlation coefficient between two parameters such as pH (X) and Electrical conductivity(Y) are calculated as

$$r = \frac{\Sigma xy}{\sqrt{X^2 + y^2}} = -0.35984$$

Where $x = X - \bar{X}$, $y = Y - \bar{Y}$, $\bar{X} = \frac{\Sigma X}{n}$, $\bar{Y} = \frac{\Sigma Y}{n}$

where n is the number of sites

For good correlation value of r should be between $-1 < r < 1$.

Calculation of Regression equation: The term regression stands for some sort of functional relationship between two or more related variables. It measures the nature and extent of correlation and predicts the unknown values of one variable from known values of another variable. Following regression equation is used to established correlation between pH and Electrical Conductivity (EC).

$$Y - \bar{Y} = b_{yx}(X - \bar{X})$$

The above equation called regression line equation of Y on X and byx called regression coefficient of Y on X and calculated as

$$b_{yx} = \frac{\Sigma XY}{\Sigma X^2}$$

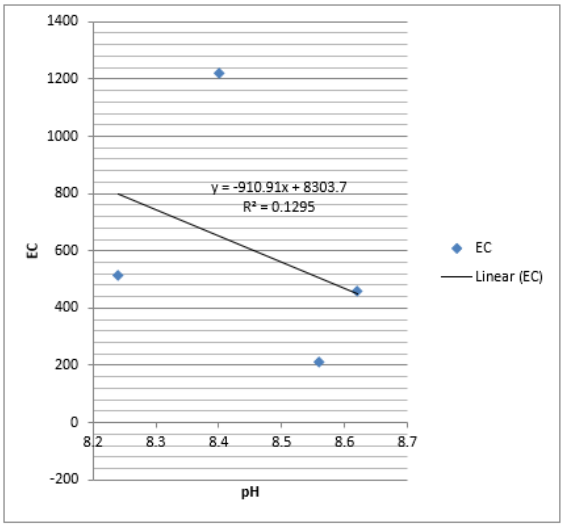

Harmful effects of pH

High pH means alkalinity. When negatively ion chemicals such as sulphate, phosphate, carbonate etc.

According to the World Health Organization, there are more harmful effects on human health when pH value is high that is when alkalinity is high. It may cause skin , eye and mucous membrane irritation.

When pH level of human body increases, this condition is known as alkalosis which can cause arrhythmia or an irregular heartbeat. This may occur when body hyperventilates.when pH level of body become high then carbon dioxide become low and sodium bicarbonate level become high. This may cause breathing rate increases and difficulty occur in breathing. Chest pain and palpitations may occur.Alkalosis can induce a coma if pH level become high. Metabolic alkalosis can cause imbalanced electrolyte levels in the body even potassium level become very low. This condition is called hypokalemia.This may lead to problems in kidneys, heart and digestive system. Respiratory alkalosis can cause seizures.

Aquatic life also suffer from pH extremes.Fish die when pH level increases above 10.

High pH level of water can corrode pipes.

Conductivity is related to the concentration of ions.These ions come from dissolved salts and inorganic materials such as alkalis, chlorides, sulphides and carbonate compounds. Compounds that dissolve into ions are called electrolytes. More ions are present more will be the electrical conductivity.

Electrical conductivity is directly related to the concentration of salts dissolve in water and therefore related to the Total Dissolved Solids (TDS). It is difficult to measure Total Dissolved Solids in the field, the electrical conductivity is used to measure the Total Dissolved Solids.

Distilled water has no dissolved ions, so it does not conduct electricity and its electrical conductivity will be zero.

Harmful effects of high electrical conductivity-

1. Disturbance of the salt and water balance in children may occur.
2. Heart and renal problems may take place.

3. Laxative effects may occur if sulphate concentrations become high.
4. Aesthetic problems of water occur with Electrical conductivity value higher than 150 ms/m and taste of water become salty.
5. It become difficult to quench thrist when value of electrical conductivity of water become higher than 300 ms/m.
6. It causes crop yield decreases.

Due to large value of Electrical conductivity activity of soil micro-organism declines so, the important microbial processes, such as nitrogen cycling, production of nitrous and other N oxide gases, respiration, and decomposition; populations of plant-parasitic nematodes can increase; and increased nitrogen losses.

6 Conclusion

From the above result and discussion it is concluded that values of pH and Electrical Conductivity of soil sample taken from site C is higher .These may have harmful effect on humans when the chemicals seep from white ash into agricultural soil and underground water such as people may suffer from alkalosis which is due to high pH and can lead to arrhythmia which means irregular heartbeat. Alkalosis can induce a coma, it may cause seizures and malfunctioning of kidneys. Due to high electrical conductivity people may suffer from heart and renal problems.

REFERENCES

[1] M. L. Jackson, Soil Chemical Analysis, Prentice- Hall of India Pvt.Ltd., New Delhi. 1967.

[2] A. K. Sinha and Shrivastava, Earth Resorces and Environmental Issues. 1st edition. ABD Publisher, Jaipur,India. 2000.

[3] B. S Patel, and H. R. Dabhi, Asian Journal of Chemistry,2009, 21(2), 1155-1158

[4] Hanlon E.A. , 2; Soil pH and Electrical Conductivity: A County Extension Soil Laboratory Manual1 ;CIR1081 Manual EDIS - University of Florida 2009.

[5] D. D. Buchholz, Soil Test Interpretations And Recommendations Handbook (1983). Revised by J. R. Brown, D.K. Crocker, J. D. Garrett, R. G. Hanson, J. A.

[6] Lory, M. V. Nathan, P. C. Scharf, H. N. Wheaton; University of Missouri – College of Agriculture, Division of Plant Sciences (5/2004).

[7] Hanlon E.A.,G. Kidder and B.L. McNeal. Soil test interpretations and recommendations. Fla. Coop. Extn. Ser.IFAS, Univ. of Fla., Gainesville, FL. CircularNo. 817. 1990,

[8] S. C. Hodges, Soil Fertility Basics- NC Certified Crop Advisor Training, Nutrient Availability and pH, (a)Chapter 10 Soil pH, Acidity and Liming and Saline, Saline-Sodic and Sodic Soils (b) Chapter 11 Salt Affected Soils (2002) .

[9] R. Rawls, American Chemical Society, 1997, pp20-22.

[10] M. Shah, P. Shilpkar, A. Shah, A. Isadara and A. Vaghela, J.Adv.Dev.Res. 2011, 2(1), 50-53

[11] A Public Discussion publication 442-508 Virginia cooperative extension, Precision Farming Tools: Soil Electrical Conductivity Robert“Bobby” Grisso, M Alley, W.G. Wysor, David Holshouser, Wade Thomason www.ext.vt.edu, 2009

[12] E.A. Hanlon, B.L. McNeal, and G. Kidder. Electrical Conductivity Interpretations. Fla. Coop. Extn. Ser., IFAS,

[13] J. L. Smith, J. W. Doran : Editors : J. W. Doran, A. J. Jones, Methods for assessing soil quality. Measurement and use of pH and electrical conductivity for soil quality analysis. 1996, pp169-185

[14] H. Kaur, “Environmental chemistry”, Pragati Prakashan, 2nd Edition, 2002.

[15] M. A. Ali, P. J. Baugh, International Journal of Environmental Analytical Chemistry, 2003, pp 923-933.

[16] Yogita Sharma and Kamalpreet Kaur, (2016) “Determination of Nitrates and Sulphates in Water of Barnala region and their Harmful effects on Human Lives”. International Journal of Advanced Research In Education and Technology. (IJARET), Vol.3, Issue 3(July-Sept.2016), 79-82

[17] Yogita Sharma, Kamalpreet Kaur and Vinesh Kumar (2016) “Textile Industries: Lead Discharge in Barnala Region, Punjab (India) - Devastating effects on Humans.” International Journal of Current Microbiology and Applied Sciences (IJCMAS), Vol.5 (9), Issue Sept., 626-634

[18] Yogita Sharma, Kamalpreet Kaur and Vinesh Kumar (2016) “Impact Of Textile Effluents on Physico-Chemical Parameters of Water In Barnala Region (Punjab,India): Risk On Human Lives”. International Journal of Advanced Research in Education and Technology (IJARET), Vol.3, Issue 3(July-Sept.2016), 116-120

[19] Yogita Sharma, Kamalpreet Kaur and Vinesh Kumar (2016) “An Assessment of Physico-chemical Parameters of Water in Barnala Region: Risk to Human Lives”. International Journal of Science Technology and Management (IJSTM), Vol.05, Issue 08 August 2016, 517-526

[20] Yogita Sharma, Kamalpreet Kaur and Vinesh Kumar (2016) “Textile Effluents Changes Physico-chemical Parameters of Water in Barnala Region: Threat for Human Lives”. International Conference on Innovative Research in Material Sciences, Energy Technologies and Environmental Engineering for Climate Change Mitigation, at Jawaharlal Nehru University, New Delhi on 25th Sept.2016

[21] Kamalpreet Kaur, Dr.Yogita Sharma and Dr. Vinesh Kumar(2018)"Cleaning of Water from Impurities by the Method of Filteration". International Journal of Research. Vol- 05, Issue-01, January 2018,pp-954-961

SOCIETY FOR SCIENCE AND EDUCATION
UNITED KINGDOM

TNC TRANSACTIONS ON NETWORKS AND COMMUNICATIONS

VOLUME 7, NO. 6
ISSN: 2054 -7420

The Effectiveness of Problem Based Learning Method on Students' Achievement in An Analog Electronics Course at Palestine Polytechnic University

Abdallah Moh'd Arman
Hebron, Palestine,
armana@ppu.edu

ABSTRACT

This study, undertaken at the Palestine Polytechnic University in Palestine, describes how problem-based learning (PBL) affects the Students' Achievement in 'analog electronics course'. Problems were designed to match real-life situations. Data of the experimental group learning outcome effects, were compared.. It was found that students who followed the PBL method learned to do research, learned better how to work in groups and developed greater confidence. Also what they learned was more of a practical value and they had more positive attitudes and reflected more. This research is in response to the real need to address gaps between employer expectations and higher education outcomes in Palestine.

In this study, an experimental group of (16) students was examined after studying a course using PBL approach. The students' achievement was examined before and after the experiment. The research results proved that there is a significant increase in gain in achievement. The PBL has achieved efficiency greater than (80%) in achievement. Also, the PBL has achieved efficiency greater than (1.2) measured with respect to Black's Gain Ratio in achievement. Also, PBL has achieved efficiency greater than (0.6) measured with respect to McGugian's Gain Ratio in achievement. The PBL has achieved larger effect size (more than 0.14) on achievement.

Keywords: PBL, Students' Achievement, pre-test, post-test, t-test

1 Introduction

Usually, engineering students have to do laboratory experiments as part of the curriculum and they should be able to apply their knowledge. According to Kitogo (2011), "today's graduates have attractive curricula vitae, but practically, their performance is insufficient; it doesn't match with what they claim to have studied". According to Case (2011), students in the lecturing mode who followed the traditional instruction are graduating with a good knowledge of fundamental engineering science and computer literacy, but they do not know how to apply that in practice. Students tend to memorize new information instead of using it as a tool to solve problems when it is presented to them without meaning or relevance in the lecturing mode and this leads to inert knowledge.

DOI: 10.14738/tnc.76.7586
Publication Date: 28th December 2019
URL: http://dx.doi.org/10.14738/tnc.76.7586

Actually, there is a great debate about whether it is the use of a particular delivery technology or the design of the instruction that improves learning (Clark, 2001; Kozma, 2001). It has long been recognized that specialized delivery technologies can provide efficient and timely access to learning materials; however, Clark (1983) has claimed that technologies are vehicles that deliver instruction, but they do not influence student achievement. Similarly, Schramm (1977) suggested that learning is influenced more by the content and instructional strategy in the learning materials than by the type of technology used to deliver instruction.

Problem-based learning (PBL) is still in the developmental stage. There is not sufficient research or empirical data to be able to state with certainty that problem-based learning is a proven alternative to other forms of learning, especially in the Arab countries. Based on evidence gathered over the past years, problem-based learning appears to be an effective model for producing gains in academic achievement. However, only a few of them have focused on problem-based learning in Electrical Engineering. Analogue electronic components and circuits are building blocks for any electronic device used in industries or in daily life. It is therefore necessary for electronics engineers to understand clearly the principles and functioning of the basic analogue components and circuits. This course will enable the students to understand the basics of construction, working, and applications of various types of electronic components such as Diodes, BJT, JFET, MOSJFET and circuits such as Small Signal amplifier, oscillators, power amplifiers, operational amplifier, and timers using linear ICs. Practical exercises of this course would enable students to maintain such circuits and in turn maintain equipment having such circuits. This course is therefore one of the basic core courses which is a must for every electronic engineer and hence should be taken very sincerely by students.

The need for this study arises from three main things: the personal experience of the researcher in teaching field, the literature review on problem-based approach and the roles of the teacher and real needs of teachers of Electronics. First, the researcher noticed that students' achievement level in Electronics courses is decreasing as they practice learning Electronics almost only inside the class or to study for the exams. As a result, the researcher tried to find a useful strategy to facilitate learning Electronics. Second, having reviewed the current literature, the researcher has figured out that the field of Electronics teaching and learning is poor in studies concerning the roles of the teacher and learners in light of the problem-based learning approach to teaching Electronics in Arab countries. Third, the unexpected low rate of success in these courses is a problem which deserves to be studied.

Employers expect more from local graduates, especially when it comes to the application of knowledge (Griesel & Parker, 2009). According to Erasmus, Loedolff, Mda, and Nel (2006), young people are unemployed or lack entrepreneurship due to a lack of specialized skills. Some of those skills are identified by Bethlehem (1997) as 'communication skills', 'decision-making skills', 'analytical skills', teamwork skills, 'well-practised leadership skills' and 'good interpersonal skills'. Many students at PPU University struggle to design an electronic project of reasonable proportion in a final year program under the label 'Design of Graduation Projects' due to a lack of application of knowledge.

Problem-Based Learning (PBL), an alternative to the traditional lecture-based approach, is built on the principle of constructivism in which learners are confronted with a meaningful authentic context. PBL originated from the McMasters University in Canada in the late sixties, using a problem-based approach

in medicine (Kolmos, de Graaff, & DU, 2009). Some European universities such as Aalborg in Denmark also implemented problem orientated, project organised PBL (Kolmos, Fink, & Krogh, 2006).

2 The research problem may be defined in the following question:

What is the effectiveness and usefulness of using problem-based learning (PBL) approach in teaching 'analog electronics course' for students of Electrical Engineering programs in the Palestine Polytechnic University (PPU)?

2.1 The Research Hypothesis

1- Problem-based learning (PBL) approach has efficiency in achievement not less than 80%.
2- Problem-based learning (PBL) approach has efficiency in achievement not less than 1.2 as measured with respect to the modified Black's Gain Ratio.
3- Problem-based learning (PBL) approach in achievement not less than 0.6 as measured with respect to the McGugian Gain Ratio.
4- Problem-based learning (PBL) approach has an effect size on achievement not less than 0.14.

2.2 The Research Methodology

The research was carried out using the experimental methodology in which the 16 student were treated as an experimental group.

3 Experimental Design

The process and purpose of the research study was explained to the students. The 16 students were randomly grouped in pairs All students were satisfied with the allocations made and no one requested to change partner. PBL requires students to work much harder than traditional lecture method.

The students were requested to solve the problem, following the operational definition of PBL according to Barrett, Mac Labhrainn, and Fallon (2005):

1. First students are presented with a problem.
2. Students discuss the problem in a small group PBL tutorial. They clarify the facts of the case. They define what the problem is. They brainstorm ideas based on their prior knowledge. They identify what they need to learn to work on the problem, i.e. what they do not know (learning issues). They reason through the problem. They specify an action plan for working on the problem.
3. Students engage in independent study on their learning issues outside the tutorial. This can include: library, databases, the web, resource people and observations.
4. They come back to the PBL tutorial(s) sharing information, peer teaching and working together on the problem.
5. They present their solution to the problem.
6. They review what they have learned from working on the problem. All who participated in the process engage in self, peer and tutor review of the PBL process and reflections on each person's contribution to that process.

The problem was stated as: assume that you are working for an Electronics company. They have asked you to design, develop and test a suitable regulated DC power supply of 9 volt , 100 mA. The line voltage 220VAC can go as low as 200VAC and as high as 240VAC from time to time, usually for small periods. Large

quantities of these power supplies are expected to be sold and you are requested to make the system as cheap as possible.

1st Small group meeting - PBL students met in their respective pairs and discussed the problem. Each student in the group had to use his/her own knowledge and experience and presume that they were personally asked to solve the problem/s. They needed to come up with a small number of hypotheses that were likely to explain and solve the problem and then divide the work to be done amongst the group members.

Individuals – They worked separately over the next 3 days to allow each member to independently carry out the research on how to design, develop, and test a suitable power supply.

2nd Small meeting - The pairs met again and drew conclusions on the nature of the problem and the best fit solutions given the information known.

Finally, each pair of students implemented the solutions, demonstrated the operation of the power supply, and submitted a report as to the solution and its consequences.

. All students had done a post-test after the experiment.

3.1 Variables Calculations and Statistical Processing

After completing the experiment, I have collected the data to be analyzed. The following relations were used in this research to measure the students' gain in achievement after studying the analog electronics course using the PBL approach.

1. Gain = posttest grade – pretest grade

2. Modified Black's Gain Ratio:

Modified Black's Gain Ratio = (Y-X)/(D-X) + (Y-X)/D

Where: Y = grade of post-test

X = grade of pre-test

D = test maximum grade

This ratio interval is [0, 2] and the instructional program is considered acceptable if the computed ratio is not less than 1.2, (Roebuck, 1973, p 472-473).

3. McGugian Gain Ratio:

McGugian Gain Ratio = Real Gain/Expected Gain

McGugian Gain Ratio = (Y-X)/(P-X)

Where: Y = average of post-test grade

X = average of pre-test grade

P = test maximum grade

This ratio interval is [0, 1] and the instructional program is considered acceptable if the computed ratio is not less than 0.6, (Roebuck, 1973, p 472-473).

4. Effect Size: How much change the independent variable will affect the students' achievement and attitudes in studying a new program.

In this research I mean how much change the PBL approach will affect the students' achievement in studying the course.

Statistically, the square of eita (ŋ2) will be used. Ŋ = t2/(t2 +df) , t-value with degrees of freedom df. This factor should be greater than 0.14

5. Descriptive Statistics.

6. t-test: The t-distribution is a bell-shaped, symmetric about the mean distribution, used when the sample size is less than 30 and the variance is normally or approximately normally distributed. It is actually a family of curves based on the concept of degrees of freedom, which is related to sample size (df = n-1). As the sample size increases, the t-distribution approaches the standard normal distribution.

4 Results

When examining descriptive data concerning the pretest and posttest achievement scores (table 1), it was noticed that there is an increase in the mean of scores by (55.2) after the application of the PBL method. This value represents the gain in students' achievement.

When examining descriptive data concerning the pretest and posttest achievement scores (table 1), it was noticed that there is an increase in the mean of scores by (55.2) after the application of the PBL method. This value represents the gain in students' achievement.

4.1 Paired Samples Statistics

To check the validity of the first hypothesis, the paired samples (dependent) t-test was run on the SPSS-15 program to determine any significant differences between post- and pre- test scores. The results are shown in table (1). It is clear from this table that the mean in the scores is increased from (30.30) to (85.50) by a difference of (55.20).The computed t-value equals (6.127) at degree of freedom equals (15) with statistical significance less than (0.001). This is less than the claimed level of significance α (0.05), therefore the null hypothesis is rejected and the alternative hypothesis is accepted i.e. there is significant differences at level of α (0.05) between the mean scores of the achievement of pretest and posttest, favoring the posttest).

Table 1: Achievement Dependent Samples t- test

Achievement	N	Mean	Std. deviation	t-value	df	p-value
Pretest	16	30.30	9.66	6.127	15	0.001
Posttest	16	85.50	4.91			

4.2 One-Sample t-test

To check the validity of the second hypothesis the one-sample t-test was run to determine whether a difference exists between the posttest scores after application of PBL on the course and the test value of (80%). The results are shown in table (2).The computed t-value equals (1.535) at degree of freedom equals (15) with statistical significance (0.149). It is clear that there is no significant difference between the

posttest scores and the degree 80% (posttest mean = 85.5).Therefore the null hypothesis is accepted i.e. PBL has efficiency in achievement not less than 80%.

4.3 Achievement Black's Gain Ratio

To check the validity of the third hypothesis ,the gain is calculated for each student based on the equation specified in section (3.1). The mean and standard deviation of this gain is calculated and shown in table (3). It is clear from this table that the calculated mean of Black's Gain Ratio equals (1.29) which is greater than the reference value (1.2). This implies that PBL achieves efficiency greater than Black's Gain Ratio.i.e. Accepting the null hypothesis.

Table2:One Sample test

	Test Value = 80					
Achievement	**N**	**Mean**	**Standard deviation**	**t-value**	**df**	**p-value**
Posttest	16	85.5	4.91	1.535	15	0.149

Table 3: Achievement Black's Gain Ratio

	N	**Minimum**	**Maximum**	**Mean**	**Std. Deviation**
Black's Gain	16	1.22	1.41	1.29	.05771

4.4 Achievement McGugian Gain Ratio

To check the validity of the forth hypothesis ,the gain is calculated for each student based on the equation specified in section (3.1). The mean and standard deviation of this gain is calculated and shown in table (4). It is clear from this table that the calculated mean of McGugian Gain Ratio equals (0.76) which is greater than the reference value (0.6). This implies that PBL achieves efficiency greater than McGugian Gain Ratio.i.e.accepting the null hypothesis.

Table4: Achievement McGugian Gain Ratio

	N	**Minimum**	**Maximum**	**Mean**	**Std. Deviation**
McGugian Gain	16	.69	.89	.76	.05934

4.5 Effect Size of e-learning on Achievement

To check the validity of the fifth hypothesis The square of (η) is calculated and summarized in table (5). The square of (η) equals 0.65 which is greater than the reference value (0.14). This implies acceptance of the claimed hypothesis.

Table5: Effect Size of e-learning on Achievement

N	t-value	df	η^2	Effect Size
16	6.127	15	0.65	large

5 Conclusions

From this discussion, it is clear that PBL improves the students' achievement. It was found that students who followed the PBL method learned to do research, learned better how to work in groups and developed greater confidence. Also what they learned was more of a practical value and they had more positive attitudes and reflected more.

After the results of the research have been lighted, the researcher would like to suggest the following points:

- The PBL approach should be used in our Universities. Engineering departments who still offer engineering courses in the traditional way

should consider promoting the use of the PBL method in at least one experiment for each of the major subjects across the engineering spectrum. Participating lecturers can then be trained in the use of PBL before implementation and dedicated facilitators could also be considered. The library and internet facilities will be used more frequently when PBL is used as a learning method and future library planning should included addressing this

opportunity..

- Execute practical sessions for students of all levels concerning use of PBL.

- Encourage instructors to practice PBL approach.

REFERENCES

[1] Barrett, T., Mac Labhrainn, M., I, & Fallon, H. (2005). Handbook of Enquiry & Problem Based Learning.

[2] Bethlehem, P. A. (1997). National Association of Colleges and Employers. Job Outlook 98

[3] Case, J. M. (2011). Knowledge matters: interrogating the curriculum debate in engineering using the sociology of knowledge. Journal of Education, 51, 73-92.

[4] Clark, R. E. (2001). A summary of disagreements with the "mere vehicles" argument. In R. E. Clark (Ed.), Learning from media: Arguments, analysis, and evidence (pp. 125-136). Greenwich, CT: Information Age Publishing Inc, http://homepages.hvu.nl/ilya.zitter/References.htm.

[5] Clark,R E. (1983). Reconsiderig research on learning from media Review of Educational Research 53(4), 445-459

[6] Erasmus, B. J., Loedolff, P. v. Z., Mda, T. V., & Nel, P. S. (2006). Managing training and development inSouth Africa (5 ed.). Southern Africa: Oxford University Press

[7] Griesel, H., & Parker, B. (2009). A baseline study on South African graduates from the perspective ofemployers - Graduate Attributes. South Africa: Higher Education South Africa & The South African Qualifications Authority Retrieved FROMhttp://www.saqa.org.za/docs/pubs/general/graduate_attributes.pdf.

[8] Kitogo, A. S. (2011). How competent are Tanzanian graduates? . Retrieved 28/11/2011, from http://varsitycollegetz.ning.com/profiles/blogs/how-competent-are-tanzanian-graduates.

[9] Kolmos, A., de Graaff, E., & DU, X. (2009). Diversity of PBL - PBL Learning Principles and Modules. In X. DU, E. de Graaff & A. Kolmos (Eds.), Research on PBL Practice in Engineering Education (pp. 9-21).Rotterdam: Sense Publishers.

[10] .Kozma, R. B. (2001). Counterpoint theory of "learning with media." In R. E. Clark (Ed.), Learning from media: Arguments, analysis, and evidence, ISBN: 1930608772, (pp. 137-178). Greenwich, CT: Information Age Publishing Inc

[11] Kolmos, A., Fink, K. F., & Krogh, L. (2006). The Aalborg PBL model - Progress, Diversity and Challenges Vol. 1. (pp. 393). Retrieved from http://www.bog-ide.dk/productsamples/9788773079119.